

Tracking activity patterns of a multispecies community of gymnotiform weakly electric fish in their neotropical habitat

Jörg Henninger, Fabian Sinz, Rüdiger Krahe, Jan Benda

August 7, 2018

Abstract

Tracking the behavior of freely roaming and untagged animals in natural environments is notoriously challenging. Weakly electric fish with their continuously active, individual-specific electric organ discharge are ideal subjects for monitoring undisturbed individual behavior. We here present automated, EOD-based tracking allowing to discern presence and movement of multiple fish simultaneously. Monitoring a multi-species community of electric fish in their natural habitat, we reveal diurnal activity patterns and provide an unprecedented window into the so-far hidden life history of weakly electric fish, making electric fish highly accessible for tackling new research questions from the areas of behavioral ecology, evolution, and neuroscience.

[RK: Vielleicht könntest du in Abstract und Intro noch mit reinnehmen, dass du das System durch kontrollierte Messungen und Simulationen überprüft/kalibriert hast.]

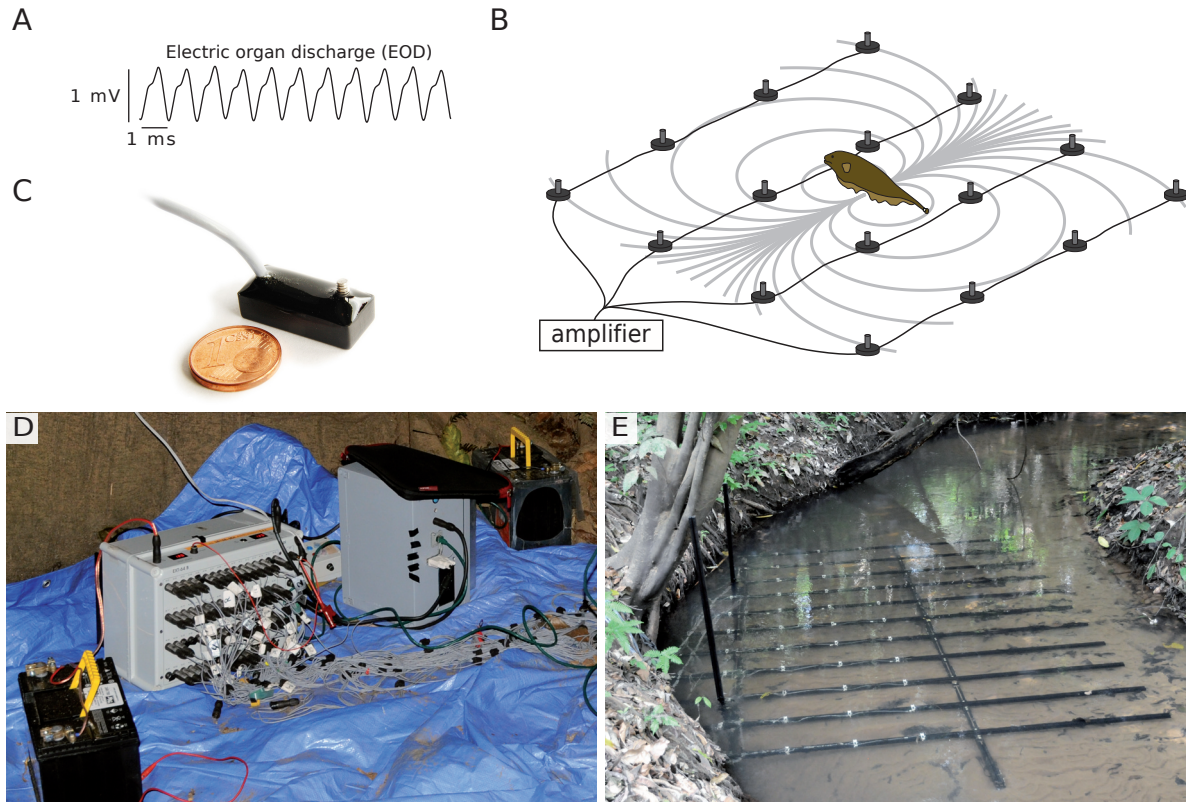
Introduction

Tracking the behavior of freely roaming and undisturbed animals in natural environments is notoriously challenging (Rodriguez-Munoz et al., 2010). E.g. ... *[EXPAND ON OUTDOOR BEHAVIOR IN VARIOUS ANIMALS AND SHOW THE DIFFICULTIES!]* *[JB: Also check Ian Couzin and Adriane Strandburg]*

Gymnotiform wave-type electric fish generate weak (~ 1 mV/cm), continuous electric organ discharge (EOD; Fig. 1 A) starting from a few days after hatching until eventual death. The EOD is an integral part of an active electrosensory system that — complemented by a large number of electroreceptors distributed over their skin — is used for diverse functions such as prey capture (Nelson and MacIver, 1999), navigation (Fotowat et al., 2013b), and communication (Smith, 2013). The frequency of electric organ discharges (EOD f) is species and individual-specific and remains in constant environments remarkably stable over many hours and days (Bullock, 1970; Moortgat et al., 1998), providing individual frequency tags ideally suited for individual recognition. The electric currents generate a non-uniform, approximately dipolar shaped electric field surrounding the fish's body (Fig. 1 B).

[JB: Cite the few outdoor papers and conclude that nocturnal and continuously recorded activity of weakly electric fish is missing.]

We here present an automated approach for EOD-based tracking of electric fish. Sensitive electrodes spread out over their habitat pick up frequency and intensity of their electric fields and allow to infer identity and movements of untagged and undisturbed individuals (Fig. 1 B E; Hagedorn and Heiligenberg, 1985; Henninger et al, 2017). We monitored a multi-species community of weakly electric fish in a small stream in Darién, Panamá, and quantified individual EOD characteristics and population-specific movement patterns.



1.4 MB

Figure 1: Recording electric fish in their natural habitat. A) Quasi-sinusoidal EOD waveform of *A. rostratus* ($\sim 580 - 1100$ Hz). B) The EOD generates a dipolar electric field (gray isopotential lines) that we recorded with an electrode array. C) Electrode headstage. The actual electrode is the stainless-steel screw on the right. D) 64-channel amplifier (grey box to the left) and recording computer (right box) powered by two 12 V car batteries (black with yellow handle). E) The electrode array at our recording site in a small stream in Darién, Panamá. White plastic holders keep the headstages (panel C) in place. Electrodes were positioned partly beneath the excavated banks, allowing to record electric fish hiding deeply in the root masses.

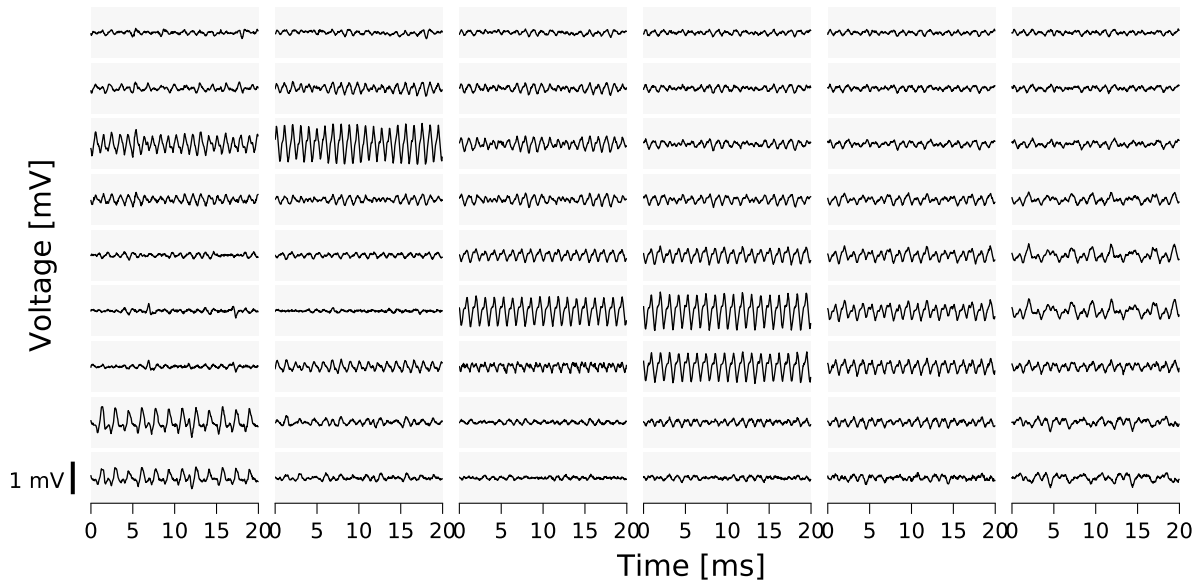


Figure 2: Raw electrode data. Each of the 54 gray boxes shows the recorded voltage of each of the electrodes as they are arranged in the grid. Three *A. rostratus* are concurrently present, a low frequency female (lower left) and two high frequency males (upper left and center). The EODs of the fish are captured simultaneously by multiple electrodes in their vicinity.

35 **Results**

36 **Recording weakly electric fish with a grid of electrodes**

37 The potentials of the electric fields generated by weakly electric fish are in the millivolt range and below. We
 38 used low-noise headstages encased in epoxy resin for each electrode as buffer amplifiers to keep the impact of the
 39 electrodes on the electric fields small (Fig. 1 C). A 64-channel amplifier filtered, amplified, and digitized the signals
 40 that were then written on a harddrive. The whole system was powered by car batteries (Fig. 1 D).

41 The electrodes were arranged in a grid and mounted on a rigid polymer frame (240×150 cm). The grid was
 42 submerged in a small stream in Darién, Panamá about 30 cm below the water surface such that it covered the cut
 43 bank side inclusively the washed out root masses where the fish hide during the day (Fig. 1 E). The electrodes were
 44 spaced by 30 cm, about two to three times the body length of the fish.

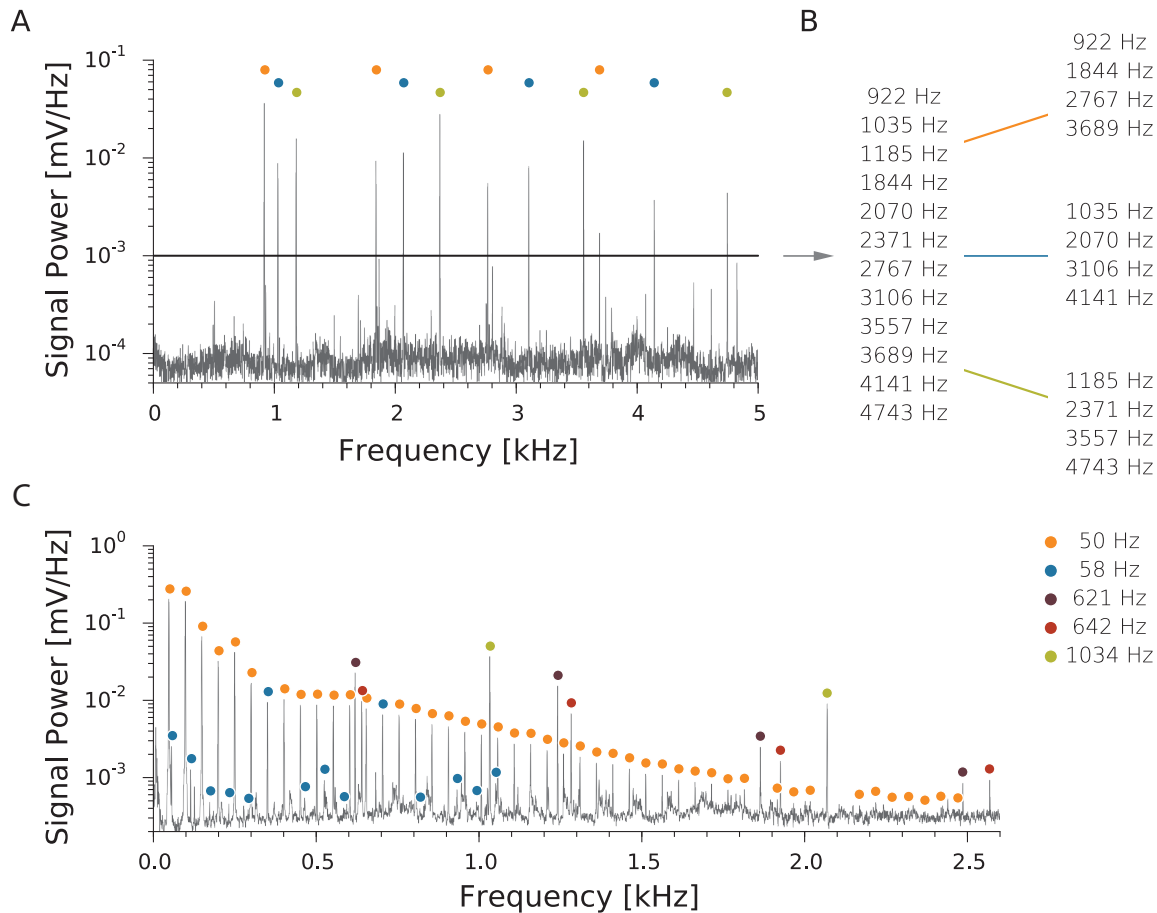
45 This setup allowed us to record the weak electric fields generated by the fish with high quality. The electric
 46 fields of fish within the recording array were commonly picked up by several electrodes simultaneously (Fig. 2).

47 **Identification of individual electric fish by EOD frequency**

48 Species and even individual fish differ in the frequency of their EODs. By extracting the EOD frequency from
 49 the raw data we therefore can identify individual fish. This conceptionally simple task is complicated by the fact
 50 that in general more than a single fish is picked up by an electrode. Furthermore, because EOD waveforms are
 51 distorted sine waves (Fig. 2 A), the resulting frequency spectra of individual fish contain harmonics, i.e., peaks at
 52 multiples of the fundamental EOD f . Together this results in complex frequency spectra where peaks originating
 53 from individual fish are intermingled (Fig. 3 A, C).

54 Moreover, the amplitude of the EOD-related peaks in the spectrum depends on distance and relative orientation
 55 of fish and electrode. *[JB: Why does this complicate the detection of fundamental frequencies? Do you mean*
 56 *the relative amplitudes of harmonics?]* *[JH: Yes. I will reformulate this.]*

57 We solved this problem by analyzing the frequency spectra for periodically occurring frequency peaks (i.e.,



[JB: unit of signal power is mV^2/Hz] [JB: Make frequency lists in B flush to the right, add titles: “all peaks”, “fish 1”, “fish 2”, ... or something like this] [JB: Rearrange: C (to show that spectra are complicated), A+B (harmonic groups)]

Figure 3: EODs are detected based on their spectral representations. A) FFT spectrum of the EODs of three concurrently present electric fish. B) Peak detection generates a list of prominent frequencies (left), which is sorted into EOD-related harmonic structures (right). C) Spectrum of field data recorded in Darién, Panamá, representing the EODs of five concurrently present electric fish belonging to two species, the low-frequency *Sternopygus dariénsis* (< 200 Hz) and high-frequency *Apteronotus rostratus* (~ 600 – 1200 Hz). Detected EODs are displayed on the right. Colored markers mark the EODs' harmonic structures.

58 harmonics, Fig. 3 A) and grouping a spectrum's many frequency peaks into a few EOD-related harmonic structures
59 (Fig. 3 B, C).

60 For each electrode we calculated power spectral densities (PSD, 8192 FFT data points, 5 overlapping sub-
61 windows, overlap 50%, total width= 1.22 s) in subsequent analysis windows (85 % overlap). In the log-transformed
62 PSDs we detected peaks using a relative threshold for the peak height (Todd and Andrews, 1999). The frequency
63 resolution of the PSDs and peak positions was $\Delta f = 2.44$ Hz.

64 For finding conclusive harmonic structures we started with the frequency f_{max} of the peak with the highest
65 amplitude and checked whether harmonics at integer multiples of this frequency were present. As the fundamental
66 frequency is not always the strongest frequency in an EOD's PSD, we checked for harmonic structures with fun-
67 damental frequencies at integer fractions of f_{max} , i.e. $f_1 = f_{max}/n$ for a small range of integers $n \leq 4$. Because of
68 the discrete frequency resolution of the PSD the fundamental frequency has an uncertainty of $f_{tol} = \pm \Delta f/2$. In
69 practice we set f_{tol} slightly higher ($f_{tol} = \pm 0.7 \Delta f$) because peaks are distorted when riding on the flank of larger
70 peaks. When checking for harmonics at frequencies $f_i = i \cdot f_1$ this translates into frequency tolerances $\pm i \cdot f_{tol}$ that
71 grow with the order i of the harmonics. This gets rather unspecific for higher harmonics, but subsequent harmonics
72 of order i and j should also be separated by $(j - i)f_1$ with a tolerance of $2(j - i)f_{tol}$. Having identified a poten-
73 tial harmonics of the fundamental frequency we used its frequency f_i to improve the estimate of the fundamental
74 frequency via $f_1 = f_i/i$. Thus, by means of the harmonics fundamental frequencies can be estimated with higher
75 accuracy than the frequency resolution of the PSD. This updating of f_1 was stopped as soon as a predicted harmonic
76 was not present in the PSD.

77 The resulting group of harmonics was rejected if it contained less than three harmonics, if more than one of its
78 frequencies was already contained in a harmonic group of another fundamental frequency, or if more than a quarter
79 of its harmonics were not detected in the PSD. Then, the group of harmonics was compared to the so far best
80 group found for a given f_{max} and preferred if the sum of its peak amplitudes was larger and the number of missing
81 harmonics was lower. This procedure was repeated until all peaks in the power spectrum of a certain amplitude that
82 was higher than the detection threshold were considered. Finally, harmonic structures with fundamental frequencies
83 below 40 Hz, above 1500 Hz, or at the mains hum at 60 Hz were discarded.

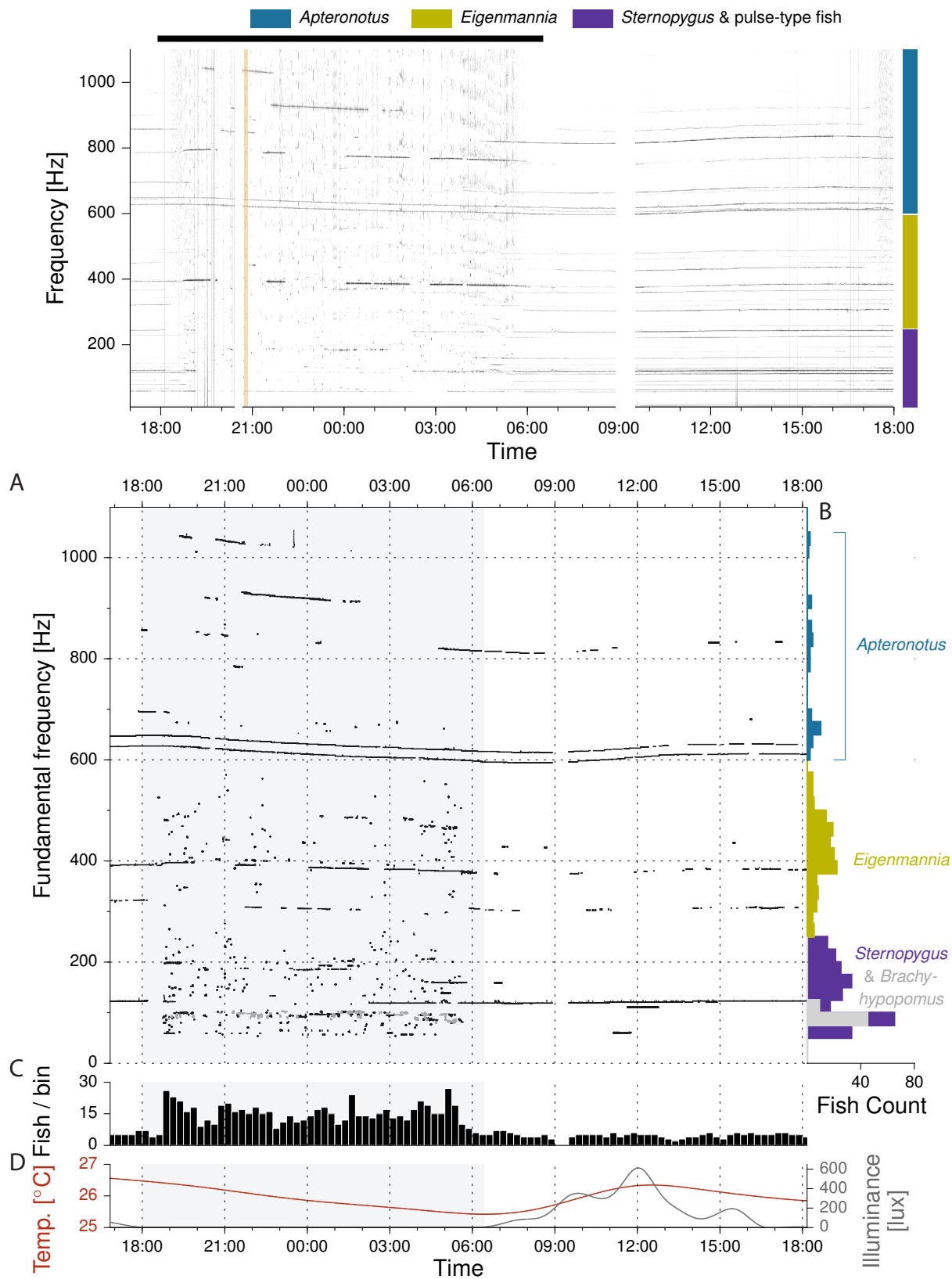
84 In a next step, individuals detected on single electrodes were matched with those of similar fundamental fre-
85 quency found on other electrodes, and finally matched over sequential time steps to generate temporal consistency.
86 This algorithm allowed us to robustly and automatically analyze large datasets containing the EODs of many elec-
87 tric fish from different species (Fig. 3 C). **[JB: this figure should be referenced for the paragraph before, it does**
88 **not show continuation]**

89 **Diurnal activity patterns**

90 The spectrogram obtained from 25 hours of an almost continuous recording demonstrates the richness and com-
91 plexity of frequencies present in a natural habitat of gymnotiform weakly electric fish (Fig. 4 A). Applying the
92 algorithm described above for extracting the fundamental frequencies allows for assessing the presence of species
93 and of individual fish over the course of the recording (Fig. 4 A). In this example we registered 461 EOD detections,
94 i.e. fundamental frequencies that were tracked in a row with possible interruptions of less than 30 s **[JB: Joerg,**
95 **what was the threshold for this?]** **[JH: Will check]**. The number of detections is presumably higher than the total
96 number of individuals, because the same fish may have left and reentered the recording area over the course of the
97 recording.

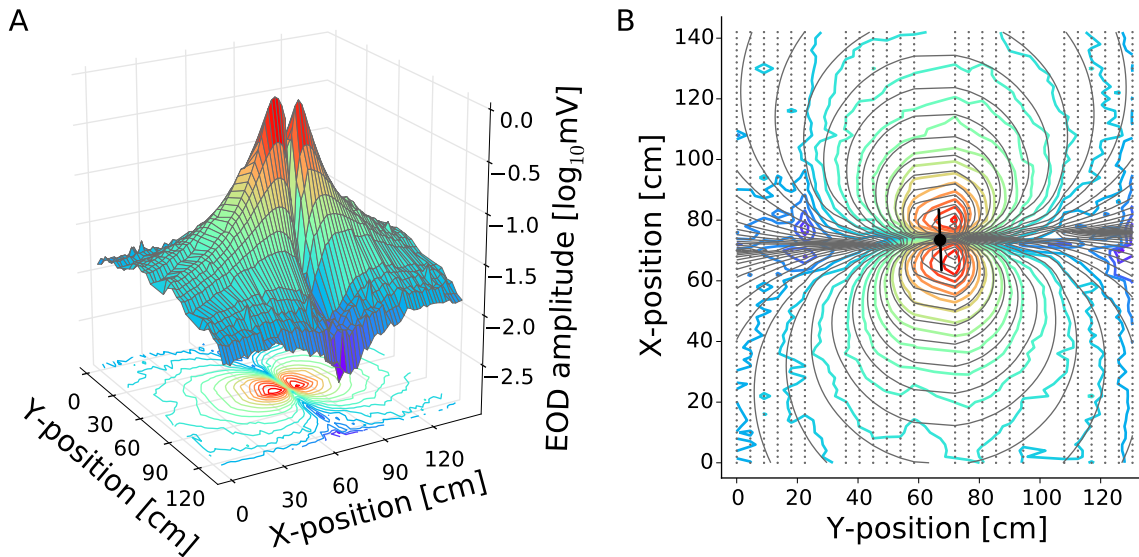
98 **[RK: Ich würde es hier noch klarer machen, dass man aus den Histogrammen nicht so einfach auf die Zahl**
99 **der anwesenden Fische schließen kann.]** A histogram of the frequencies of the EOD detections reveals three
100 distinct frequency ranges that correspond to three wave-type species (Fig. 4 B): *Apteronotus rostratus* occupied the
101 highest frequencies from ~ 580 to 1100 Hz. Right below there were *Eigenmannia humboldtii* between ~ 200 and
102 580 Hz. *Sternopygus dariensis* covered the lowest frequencies ($\sim 40 - 220$ Hz) and shared its frequency range with
103 the pulse-type fish *Brachyhypopomus occidentalis*.

104 The number of EOD detections per 15 minute time bin was on average significantly larger during the night
105 ($p = 1.1 \times 10^{-22}$, Welch's t-test; Fig. 4 C, D), confirming previous observations on the nocturnal activity of many



[JB: include the spectrogram into the figure, remove its labeling of species and day/night] [JB: What is the reddish vertical line in the spectrogram!] [JH: Previously, this indicated the position of a cutout. I will remove it when I integrate the figures.] [JB: Eventuell y-Achse von A stauchen (und dafuer C und D etwas hoeher wegen y-label?)] [JB: C ylabel: Fish / 15min]

Figure 4: Tracked electric fish over 25 hours. A) Spectrogram of the 25 hours of EOD recording tracked in Fig. 4. All channels are merged. A) Fundamental frequency traces of at least four species of electric fish. Each dot and horizontal line indicates the



[JB: can you please plot the model contour lines in B on a finer resolved grid?] [JB: what about a color bar for B?]

Figure 5: Spatial amplitude distribution of the EOD's electric field potential. A) Spatial distribution of an electric fish's EOD amplitude (absolute values). B) Dipole model (gray lines) fitted to the data shown in A.

[JB: ... the fish is positioned at (60, 60) and is oriented in the direction of the x-axis... Where is the head???)

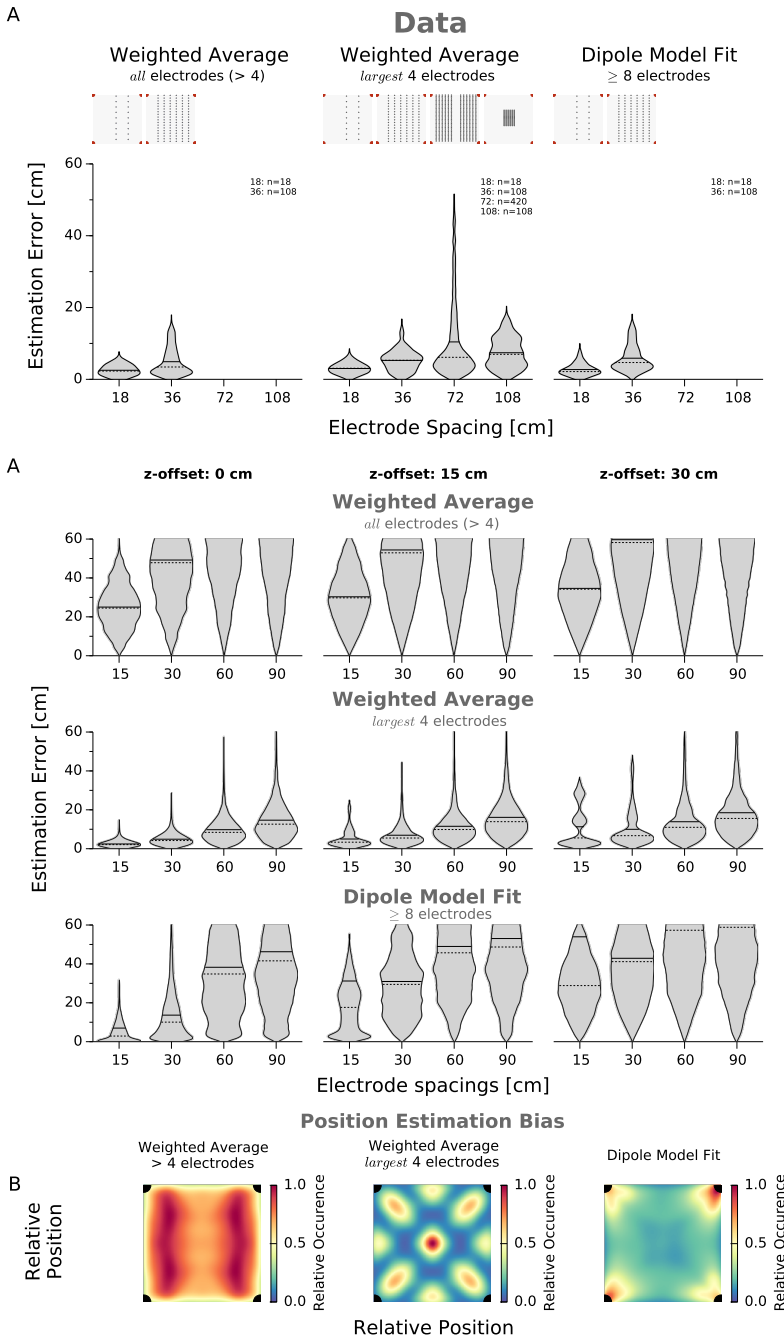
106 electric fish species **[(REF maybe Hopkins and Hagedorn)]**. The variability in the number of detected fish during
 107 the light period reflects changes in the recorded EOD signal amplitude that are presumably caused by changes in
 108 fish orientation relative to the electrode array **[JB: Was willst du damit sagen? Geht es um Fische die am Rand
 109 oder gar ausserhalb des grids sind und deshalb nicht durchgaengig getrackt werden da kleine Orientierungs und
 110 Positionsaenderungen das Signal unter irgendeine Schwellen fallen lassen???)**. **[JH: Yes, that is basically
 111 it.]**

112 EOD frequency is known to be sensitive to water temperature **[REF]**. In our recording we see that in particular
 113 the EOD frequency of *A. rostratus* is modulated by slow changes in water temperature (compare Fig. 4 D with the
 114 to fish right above 600 Hz in panel B).

115 **[JB: We might want to spell out that both EOD and movement activity are representative for other days we
 116 recorded? We would need to check that, though.]**

117 **Dipole-like far-field of EODs**

118 Crucial for studying electric fish behavior and their interactions is knowledge about each individual's position and
 119 movement over time. For defining effective layouts of the electrode array and for choosing a suitable localization
 120 approach we extended the study of Knudsen (1974) and measured the electric field's amplitude distribution over
 121 larger distances. We measured the EOD of an *Apteronotus albifrons* (18 cm length) at the center of a large outdoor
 122 tank ($3.5 \times 7.5 \times 1.5$ m, $w \times l \times h$). As expected, the spatial distribution of EOD amplitudes resembled that of
 123 an electric dipole (Fig. 5 A). The EOD amplitude was attenuated with distances from the electric fish and was
 124 modulated in dependence on the angle relative to the body axis of the fish. Perpendicular to the fish's body axis
 125 the potential was close to zero. A modified dipole, Eq. 3, fitted to the data resulted in a good description of the
 126 measured EOD amplitudes (Fig. 5 B) with an exponent $q = XXX < 2$ and an dipole moment $P = XXX$. **[JB: Fit
 127 results: amplitude and exponent as in Figure 10!]**



[JB: Merge the two figures! estimation_quality: cut estimation error at 40 cm to make it less high. sim_estimate_performance_Panama-grid: reduce width of A and place B upright on the right side. Fix caption.]

Figure 6: Evaluation of position estimation algorithms based on EOD measurements. The top row depicts the fish locations evaluated in the center quadrant of the electrode array. The violin plots in the bottom row show the distribution localization errors for different electrode spacings and algorithms. Simulation-based evaluation of position estimation for the electrode configuration deployed in the field. A) Distribution of localization errors for different electrode spacings and algorithms. B) Inherent biases of localization algorithms averaged over all quadrants of the electrode array.

128 ***EOD-based localization of electric fish***

129 Next, we evaluated the performance of three algorithms for estimating fish position based on the spatial EOD
 130 amplitude distribution based on the data described in the previous section as well as simulations. A simple estimate
 131 of 2D fish location and orientation is based on a spatial average of electrode positions weighted by the EOD
 132 amplitudes measured at the electrodes. In one version we used all available electrodes to compute the fish location,
 133 and in another version only the four electrodes with the largest EOD amplitudes. The third method fits a dipole
 134 model to the measured EOD amplitudes (see methods for details).

135 When applied to the measurement where the fish is positioned in the center and at the level of the electrode
 136 grid, all three estimators perform reasonably well with position errors mostly below 20 cm, i.e. the body size of
 137 the fish (Fig. 6 A). Increasing the distance between electrodes from 18 to 108 cm resulted in a minor increase of the
 138 median estimation error from about 5 to 10 cm.

139 In reality, however, fish may swim at various levels above or below the plane of the electrode array. In addition,
 140 they will also be located close to or even beyond the borders of the electrode array. We therefore tested the per-
 141 formance of the three position estimators in extended simulations, where we varied the static position, orientation,
 142 and level above the electrode array as well as the electrode spacing (Fig. 6 B). In these scenarios, the weighted
 143 spatial average that uses the four electrodes with the largest EOD amplitudes turned out to yield the most robust
 144 results with the lowest errors. Fitting the dipole model required narrow electrode spacing and deteriorated dra-
 145 matically for fish swimming outside the plane of the electrode array. Using data from all electrodes of the array
 146 for the weighted-spatial-average estimate resulted in errors of the same size as the electrode spacing. Only when
 147 using the four electrodes with the largest EOD amplitudes was the position estimate of the weighted spatial average
 148 largely independent of the level above the electrode array and much smaller than the electrode spacing. Although
 149 this estimate does not relate to the underlying physics of the electric field, it proved to be the most robust against
 150 interference by electrical noise and fish moving close to the edges of the electrode array. We therefore use this
 151 measure for all further analysis.

152 Additional to position, fish orientation can be estimated by taking advantage of the dipolar nature of the fish's
 153 electric field: the EOD at the head is of opposite polarity to the EOD at the tail of the fish. We divided the electrodes
 154 into two subgroups of opposite polarity and determined the direction vector between the estimated centers of these
 155 two groups as the orientation of the fish (see methods). Note, however, that with this method we cannot differentiate
 156 between the head and the tail of the fish, therefore orientation can only be estimated modulo 180°.

157 ***Position and orientation estimates of moving fish***

158 So far we tested the algorithms for position estimation on static fish only. However, fish do move, and therefore we
 159 need to also check how position estimation performs with moving fish. We simulated a fish moving with a speed
 160 of 10 cm/s (Nelson and MacIver, 1999) along a circular trajectory positioned off-center in relation to the electrode
 161 array in order to sample many different fish-to-electrode configurations.

162 The mean and mode of the position errors were clearly below 10 cm (Fig. 7 A), which corresponds to a small-
 163 sized, mature *Apteronotus* (Dunlap, 2002; Triefenbach and Zakon, 2003). Likewise, mean and mode of the orien-
 164 tation error were small and clearly below 15°. The weighted spatial average cannot follow fish positions outside
 165 the boundaries of the electrode array. Therefore the error of the position estimate increases as soon as the fish
 166 trajectory extends beyond the electrode array (Fig. 7 B). For fish trajectories vertically offset from the grid plane,
 167 the mean and spread of the localization error slightly increased, while the orientation error remained almost un-
 168 changed (Fig. 7 C). In summary, the simulations demonstrated that our algorithms are suited for tracking electric
 169 fish moving within the electrode array's limits with acceptable uncertainty.

170 ***Multi-species community***

171 *[JB: New figure: 8B plus histograms of deltafs per species]*

172 Fig. 4

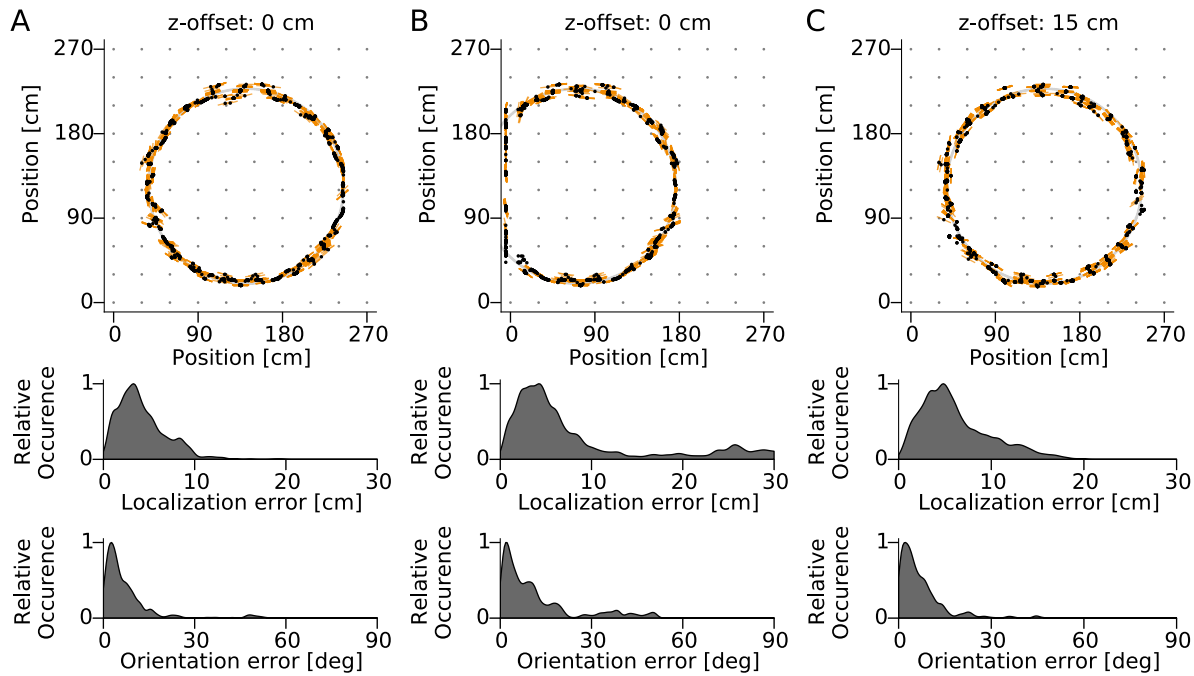
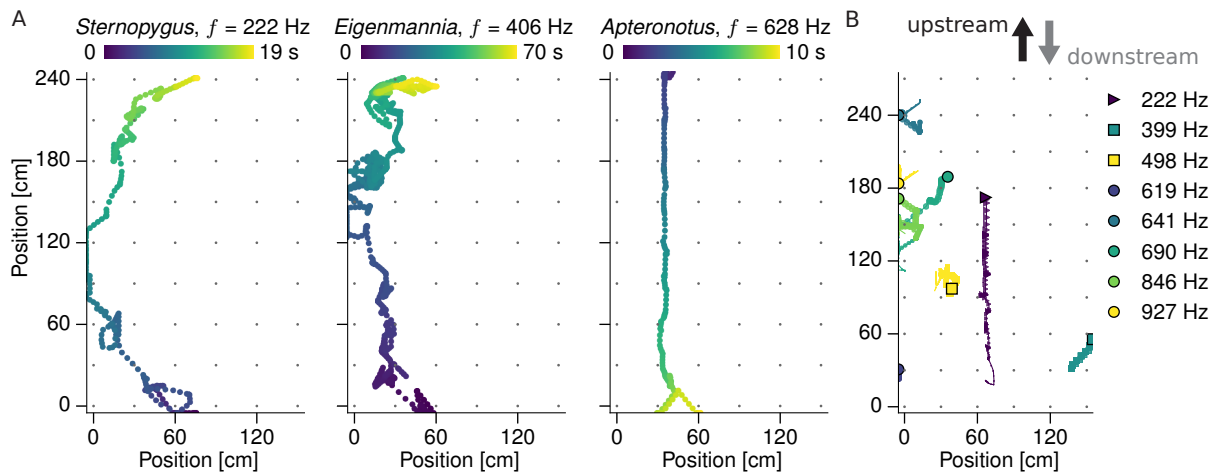


Figure 7: Evaluation of position and orientation estimates of simulated moving fish. Top: The estimated, non-smoothed 2D-locations (black dots) and orientations (orange lines) were compared to the simulated fish locations (gray line) and orientations. Center and bottom: Error distributions of localization and orientation estimation. A) Simulated movement on level with the electrode array. B) Movement on level with the electrode array, but partially outside the recording array. Errors include the difference to the known fish location and orientation for the time period the fish moves outside the array. C) Simulated movement 15 cm above the electrode array.



[JB: 1.2 MB] [JB: B is narrower than the rest] [JB: Exchange panel A and B] [JB: Mention date and time of the snapshots!]

Figure 8: Field data examples of electric fish movement. A) Left to right: A *Sternopygus dariensis* female, an *Eigenmannia humboldtii*, and an *Aptereronotus rostratus* female traversing the electrode array. Traces have been smoothed with a running average filter (width=0.2 s). B) Example of multiple concurrently present individuals of three species. Legend indicates species and EOD fundamental frequency. Triangle: *S. dariensis*, squares: *E. humboldtii*, circles: *A. rostratus*.

173 An example for the performance of our fish identification and tracking (Fig. 8 A)... Multiple species at the same
174 time present in the recording area and close by.

175 Fig. 8 shows field data examples of fish traversing the electrode array. Fish from three species were selected
176 to demonstrate that spatial tracking with a high temporal resolution is possible independent of the fish's EOD f .
177 While it is not possible to verify the validity of the shown trajectories by means of synchronously recorded videos,
178 the overall movement patterns and speed appear plausible in comparison to the simulations shown in Fig. 7 and
179 known gymnotiform fish movement speeds (up to 50 cm/s: Reardon, Satenstein, Chapman, Krahe, pers. comm.
180 XXX; Nelson and MacIver, 1999), and are in full agreement with the EOD dynamics observed on the electrode
181 recordings.

182 [RK: fish movement speed: Nelson & MacIver 1999; wir sitzen noch auf einem halbfertigen Manuskript
183 mit critical swim speeds für eine Reihe von Gymnotiformen. Unter Umständen könnten wir auch Reardon,
184 Satenstein, Chapman, Krahe, pers. comm zitieren.]

185 **Movement patterns**

186 The ability to track individual movement enabled us to study species-specific movement patterns. From the 461
187 electric fish detections over 25 hours a subgroup of 173 detections showed clear directed movement by traversing
188 the recording area within 5 to 60 seconds (Fig.9). [JB: CHECK OUT THE EXACT CRITERIA FOR THE SE-
189 LECTION OF FISH TRAVERSING THE GRID] Movement activity sets on sharply after nightfall. Individuals
190 of all species had a strong tendency to move upstream in the first half of the night and downstream in the second
191 half, a pattern most pronounced in the larger populations of *Sternopygus* and *Eigenmannia*. A large fraction of
192 the *Eigenmannia* population returned downstream only shortly before dawn. We quantified the average movement
193 speeds of the tracked individuals (median upstream $v = 19.4, 19.2, 15.7$ cm/s for *Sternopygus*, *Eigenmannia*, and
194 *Aptereronotus*, respectively). [RK: Kannst du was dazu sagen, wie vollständig wir die auf- und abschwimmenden
195 Fische erwischt haben? Mein Gefühl ist, dass auf der Gleithangseite höchstens ganz wenige am Grid vor-
196 beigeschwommen sind. Vielleicht geben das aber auch die Daten her: Verteilung der Fische im Grid von der
197 Prallhangseite zur Gleithangseite.] [JB: Simply make a histogram of the x-coordinate, and then let's discuss

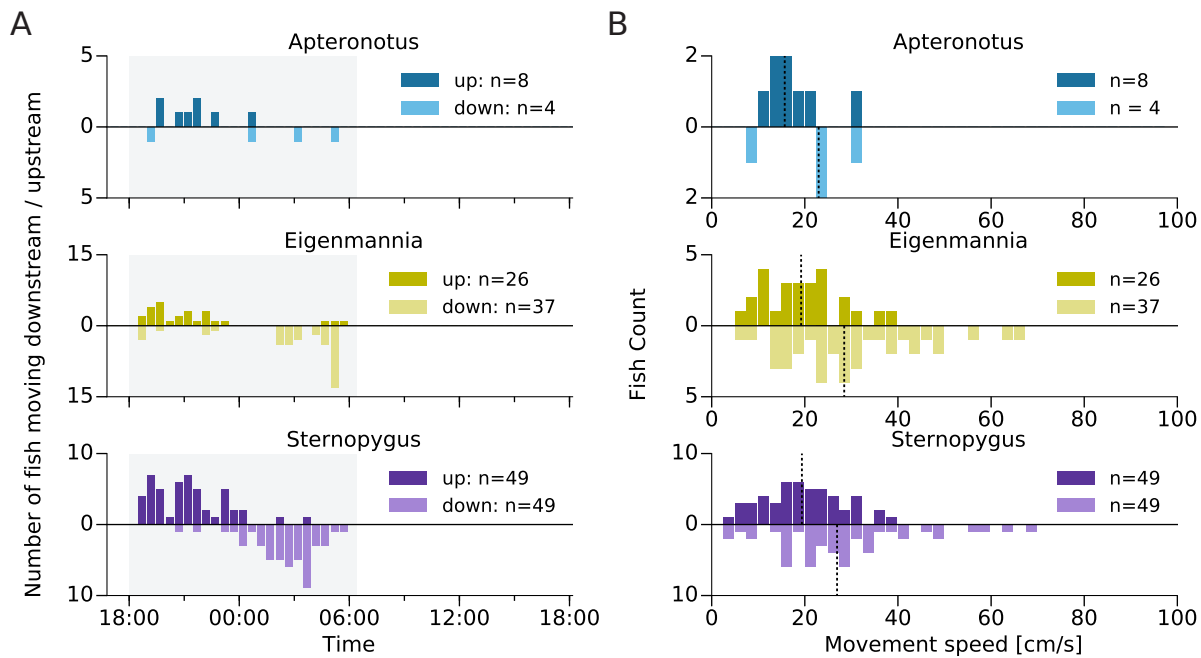


Figure 9: Summary of wave-type fish movement over 25 hours. A) Movement activity of *Aptereronotus*, *Eigenmannia*, and *Sternopygus*. B) Movement speeds of fish traversing the grid. Dashed lines indicate median speeds. **[JB: Say how many males and females of *Aptereronotus* are migrating.]**

198 **what to do with it.]** We found that, as might be expected, upstream movements were slower than downstream
 199 movements for all species (median $\Delta v = 7.6, 9.3, 7.3$ cm/s for *Sternopygus*, *Eigenmannia*, and *Aptereronotus*, re-
 200 spectively), suggesting a distinct influence of the stream's water flow on absolute swim speed. **[JH: Should we**
 201 **do statistical comparisons between species? e.g., ANOVA or t-test][JB: Ja, mach mal einfache pairwise t-Tests]**
 202 Apart from the described subgroup of fish moving in a distinct direction, a large fraction of detected fish remained
 203 resident over longer periods or did not show clear directionality. Knowledge of swim speeds allowed to estimate
 204 the distances travelled by roaming fish during the dark period. We used the median swim speeds and the half-times
 205 of upstream and downstream movements to calculate a conservative estimate. We estimated the median distance
 206 roamed by the fish to be about 3.0 km and 2.3 km for *Eigenmannia* and *Sternopygus*, respectively (unidirectional
 207 distance, not considering interruptions for foraging and social interactions as mating etc.). Due to the small number
 208 of individuals, we omitted an estimate for *Aptereronotus*. **[JB: What is the estimated water velocity for all three**
 209 **species? Is this reasonable?]** **[JH: This is written a few lines above: the median Δv]**

210 **[RK: Kannst du anhand der EODfs was zur Geschlechterverteilung bei den Aptereros sagen? Ich würde ja**
 211 **spekulieren, dass die Weibchen stationärer sind als die Männchen.]**

212 **[JB: Use recordings from the other days to improve statistics of movements; no need to manually connect**
 213 **individual fish!]**

214 **Estimation of EOD amplitudes** An important aspect of electric fish interactions are the effective signal inten-
 215 sities occurring during these interactions, which are determined by the individual EOD intensities and their spatial
 216 distribution. The distribution of EOD field intensities over the electrode array allowed us to infer the intensity and
 217 effective decay over distance of EODs under natural conditions, provided that a fish's location is known. Fig. 10 A
 218 illustrates the distribution of EOD amplitudes extracted from the voltage recordings shown in Fig. 5 **[JB: This is**
 219 **albifrons in the munich outdoor tanks]**. Because of the dipolar shape of the electric field, small EOD intensities
 220 occur even at short distances. However, the largest EOD intensities recorded at a given distance clearly decrease
 221 over distance following a power law. To extract the maximum amplitudes, data were binned logarithmically over

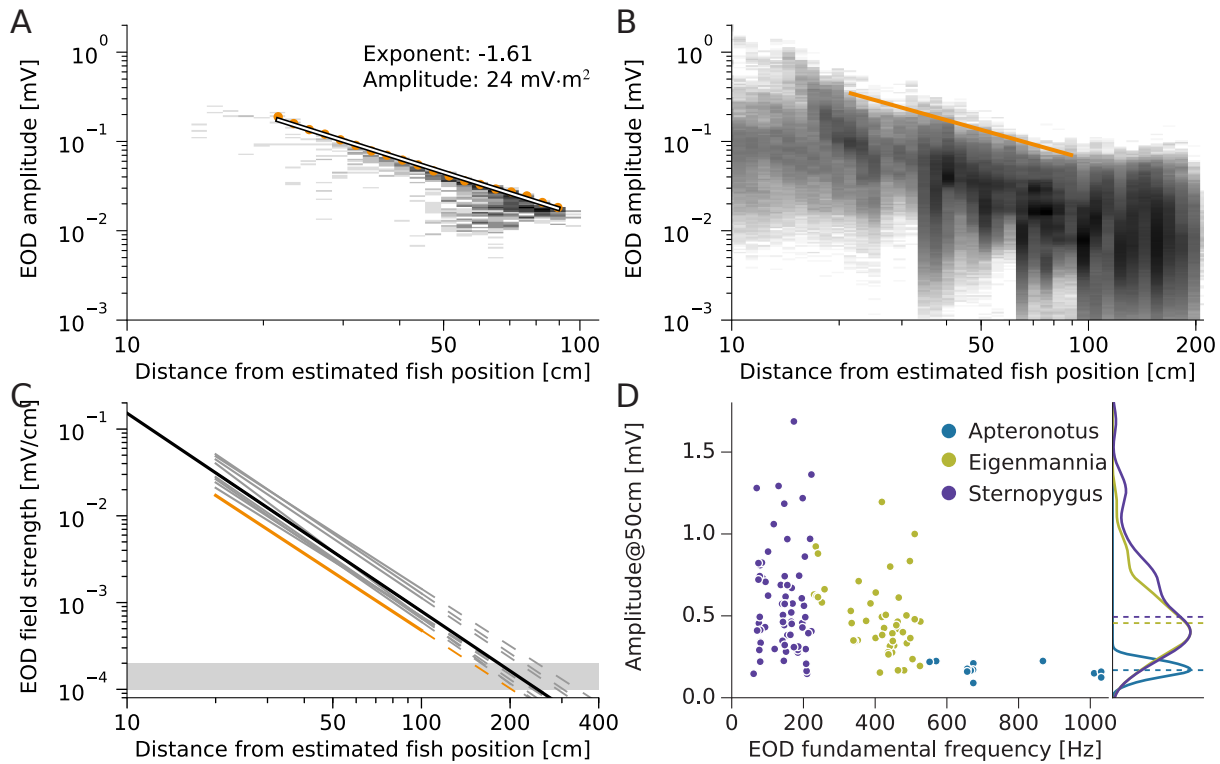


Figure 10: Estimation of EOD field strength and its decay over distance. A) 2D-histogram of EOD amplitudes over distance of the EOD field of an *A. albifrons* measured under controlled conditions and shown in Fig.5. Orange markers represent the mean of the largest 20% of EOD amplitudes per distance bin and were fitted with a power law function (line). B) 2D-histogram of EOD amplitudes for an example *A. rostratus* female tracked in the field. The largest 5% of EOD intensities per bin are used for the estimate. C) EOD field gradients for eight *A. rostratus* (short lines; orange: estimate from B, median curve shown in black) with behavioral detection thresholds (horizontal gray bar). D) Summary of EOD amplitude estimates for three species versus EOD frequency. *Sternopygus*, $n = 69$; *Eigenmannia*, $n = 47$; *Aptereronotus*, $n = 12$.

222 distance and for each bin a fixed fraction of largest amplitudes (dependent on the amount of available data: 20%
 223 for the tank measurements, 5% for the field data) were extracted, averaged, and fitted with a power law function
 224 (Fig. 10 A). The estimate yields values similar to those obtained with the ideal dipole model fit (Fig. 5 B), but has
 225 an inherent bias towards underestimation. [JB: *Once we have the number from the dipole we can make a more*
 226 *quantitative statement...*] [JH: *What dipole do you mean? Are you referring to the fish in Fig. 5?*] [RK: *ADD*
 227 *INFO ON CONDUCTIVITY*]

228 We applied this approach on a selection of *A. rostratus* recorded in the field (Fig. 10 B,C). [JB: *We need*
 229 *summary statistics of Amplitude and Exponent! Mean and SD for all three species*] Considering the known sensi-
 230 tivities of the electrosensory system for this species obtained from behavioral studies (0.3–0.1 $\mu\text{V}/\text{cm}$; Knudsen,
 231 1974; Bullock et al., 1972), this data allows us to estimate the effective detection range of *A. rostratus*, under the
 232 natural conditions encountered and based on median decay characteristics (see methods), to range between about
 233 153 – 248 cm (Fig. 10 C, at a conductivity of about 160 $\mu\text{S}/\text{cm}$). Similarly, we estimate the detection ranges for
 234 *Eigenmannia* and *Sternopygus* (sensitivities: 0.3 $\mu\text{V}/\text{cm}$; ?) under the same conditions to be 220 cm and 259 cm,
 235 respectively.

236 Additionally, our approach allows to compare the EOD amplitudes within and across species. For robust com-
 237 parison, we utilize the EOD amplitude estimated at 50 cm distance from the fish. Analyzing individuals from the
 238 three present wave-type species traversing the recording array during 25 hours (Fig. 9) reveals a broad distribu-
 239 tion of EOD amplitudes within each species. While *Sternopygus* and *Eigenmannia* have similar EOD amplitude
 240 distributions, *Apteronotus* EOD amplitudes are clearly smaller than the former (Fig. 10 E). None of the tested popu-
 241 lations showed a clear relationship between EOD amplitude and EOD f (Pearson's r and P-values for *Sternopygus*:
 242 -0.048, 0.695; *Eigenmannia*: -0.351, 0.015; *Apteronotus*: -0.378, 0.226). [JB: *We need summary statistics here*
 243 *as well (mean amplitude@50cm and SD, or median. What are the dashed lines in Fig 10 D?)*]

244 **Discussion**

245 We developed a new technology for tracking undisturbed and untagged individual wave-type electric fish based on
 246 their own continuously active EOD. We then applied this technology to track the movements of a multi-species
 247 community of gymnotiform electric fish in their natural habitat during breeding season and to characterize indi-
 248 vidual electric field properties. We quantified the population's nocturnal activities and revealed distinct movement
 249 patterns in the three monitored species.

250 **EOD-based individual tracking** Visual tracking of fish movement and behavior is well established for labora-
 251 tory setups (e.g., ?). These methods commonly rely on high contrast images and unobstructed line-of-sight, both of
 252 which are typically not readily available in natural habitats. In contrast, EOD-based tracking exclusively relies on
 253 the fish's own, continuously emitted signals, allows for easy individual identification over time (within the limits
 254 of EOD f resolution), and provides direct access to the fishes communication signals (?). However, while many
 255 behaviors of electric fish are exclusively electric in nature (e.g., electro-communication and the jamming avoid-
 256 ance response), direct evidence for physical interactions that could easily be tracked visually (?), and maybe even
 257 automatically, is inaccessible and has to be inferred jointly from EOD signals, context, and movement dynamics.
 258 Individual density differs strongly across species and habitats (REF? or personal observation? -> Kolumbien). In
 259 particular for species that modulate their EOD f s during social interactions individual tracking might be impaired
 260 if fish density is high and many similar EOD f s are present at the same location.

261 [JB: *Cite Fortune and Cowan paper*]

262 Rudimental EOD-based tracking of overall electric fish activity in natural habitats has been published previ-
 263 ously for wave and pulse-type electric fish (??). Additionally, for pulse-type electric fish an EOD-based method for
 264 tracking position in a shallow water tank in a laboratory setup has been published recently (Jun et al., 2013; ?). In
 265 our analysis we focused on wave-type fish, which allowed for individual identification based on their highly stable
 266 EOD f s. Jun et al. (2013) demonstrated that for pulse fish individual identification based on location at preceding
 267 timepoints is possible and we expect that such localization strategies are highly compatible with our recording

268 strategy and would allow to additionally track the pulse-type electric fish that are present in our recordings.

269 **Fish identification and tracking** EOD frequency (EOD f) is the single most important parameter for individual
 270 discrimination in gymnotiform wave-type electric fish. EOD f is mostly stable over hours and days, but is subject
 271 to temperature-related changes (Dunlap et al., 1998) and behavioral modulations both on short, medium and long
 272 time scales (sub-second: chirps; several to hundreds of seconds to hours: rises; Zakon et al., 2002; Smith, 2013).
 273 We therefore used the EOD f as an individual marker of wave-type electric fish.

274 The estimated location of a fish always referred to a fish's electric center. The center's relative position within
 275 the fish depends on the type and location of the fish's electric organ (Caputi et al., 2005), which in some species is
 276 distributed along the body axis and in others concentrated in a small area, and which is never located in the fish's
 277 front.

278 **Species-specific EOD frequency** At our field site we found three sympatric wave-type species with well sep-
 279 arated EOD f ranges. In contrast, other studies that focused on the deep waters of large tropical streams (e.g., ?)
 280 found higher numbers of sympatric species in close proximity displaying strong EOD f overlap. However, be-
 281 cause these habitats are not easy to access, it remains unclear if these species are syntopic or cluster in separated
 282 microhabitats.

283 *[JB: What does the literature say about sympatric weakly-electric fish species?]*

284 **Dipole field** (?) and others. Far field must be dipole (?). Exponent squeezed between ground and water surface
 285 (?).

286 The electric far-field of free swimming electric fish in a large body of water is well approximated by the three-
 287 dimensional ideal dipole model (Knudsen (1975) and see below).

288 Non-conducting tank walls and the water surface induce boundary effects in the electric field (Fotowat et al.,
 289 2013b), making small tanks less suited for measuring the spatial distribution of the electric field. We therefore
 290 might not hold true for the conditions occurring during EOD measurements because the water body is limited
 291 by the water surface and the stream bed or tank walls, which are known to introduce boundary effects that could
 292 change the effective exponent of the power law (Fotowat et al., 2013b; Jun et al., 2013). Therefore, we made the
 293 power law parameter q a free parameter to account for this effect.

294 **Movement patterns** We observed a clear nocturnal activity period ranging from dusk to dawn that is in agreement
 295 with previous reports (e.g., ??). *[JB: Add these references to references plus the Hagedorn chapter on *Brachyhy-**
 296 **popomus!*]* During this period we found a distinct diurnal movement pattern in three monitored wave-type species
 297 which consisted of net upstream movement in the first half and net downstream movement in the second half of the
 298 night. Based on the fishes swimming speeds we inferred the fishes potential swimming range. **XXX Can we relate**
 299 **the inferred swimming range to the length of the stream, both upstream and downstream? XXX** However, because
 300 in this study we tracked electric fish at a single location only, the true swimming range remains unknown. The
 301 potential of our technology reaches beyond this: in particular in small streams multiple recording sites that cover
 302 the full width of the riverbed would allow to detect all passing electric fish, determin swimming direction and to
 303 correlate the detected EOD f s over sequential sites to uncover the actual action ranges and to infer potential sites of
 304 interaction and foraging. This approach is particularly promising to uncover daily and seasonal migration patterns
 305 from the associated large stream to the small stream and vice versa.

306 Because it is not trivial to relate EOD f s across large time ranges, our tracking approach is inherently limited to
 307 unravel individual activity over short time periods. A possible, yet invasive extension of our approach that would
 308 allow for individual identification across longer time periods could be the combination with PIT tag implants (e.g.,
 309 ?).

310 *[JB: Check for papers on movement patterns in other fish!]*

311 **Amplitude versus EOD_f Correlations** ...? [RK: Bennett (1971) könnte was zu Amplituden von verschiedenen
 312 Arten haben. Wir wollen sicher einen Absatz über natural sensory stimuli/scenes. Das sollte dann aber auch
 313 aus der Überschrift des Absatzes hervorgehen (nicht einfach "data on natural pops")]
 314 [JB: Cite paper about EOD amplitudes of various species. Relation with conductance.]

315 **We need behavior** [JB: Cite and discuss the various perspective papers. Joerg has another one.] With this type
 316 of data we uncovered unexped stimulus regimes (?). Use natural data as inspiration for more specific laboratory
 317 experiments.

318 **Natural sensory scenes** XXX This paragraph is currently more of a placeholder... XXX A fact often stated by
 319 neurophysiologists working on *A. leptorhynchus* is that the characteristics of natural electric signals are well known.
 320 This view is founded on a plethora of laboratory studies, some describing the dependence of chirping on a range of
 321 parameters of EOD mimics (e.g., ?), others the influence of hormones (e.g., Dunlap, 2002) and some the chirping
 322 during staged encounters (e.g., ??) and courtship (Hagedorn and Heiligenberg, 1985). Although some studies
 323 provided very elaborated naturalistic environments (e.g., ?), all of these experiments were performed on captive
 324 fish in tanks compiled into an artificial community. In contrast, much fewer field studies on the natural behavior
 325 of gymnotiform electric fish are cited, and here mostly the works of Carl Hopkins (????), Mary Hagedorn (??),
 326 and Schwassmann (??). These works revealed much about ecology, life history and species specific distributions
 327 of EOD_f of gymnotiform fish. However, because most of these studies were both very labor intensive and yet
 328 restricted in their means to monitor the behavior of free roaming fish, and therefore many observations remain
 329 anecdotal. Our automated monitoring approach provides the means to build a quantitative foundation for natural
 330 electric signals and the interactions of the fish generating them.

331 The recording strategy of our monitoring approach can readily be adapted to the needs of larger scale studies
 332 on, e.g., the evolution and ecology of electric fish. E.g., spatial resolution can be trade-off against the size of
 333 the monitored area, or number of channels and samplerate could be traded against recording time to allow for
 334 monitoring larger areas for longer periods of time.

335 In conclusion, our study demonstrated that EOD-based, species-independent tracking of electric fish, proposed
 336 as early as 1985 by Hagedorn and Heiligenberg, is indeed possible and yields a plethora of valuable information
 337 on the monitored individuals and their populations.

338 **Materials and Methods**

339 **Measurement of spatial amplitude distribution**

340 We performed calibration recordings in a large outdoor tank ($3.5 \times 7.5 \times 1.5$ m, $w \times l \times h$). We used a 4×4
 341 electrode array mounted on a PVC frame and spaced at 36 cm (108×108 cm, Georg Fischer GmbH, Albershausen,
 342 Germany). Water depths was adjusted to 60 cm, conductivity to $150 \mu\text{S}$, and temperature to 23.5°C . A weakly
 343 electric fish (*A. albifrons*, 18 cm) was carefully placed in a fish holder made of fine nylon mesh, which was then
 344 fixed horizontally in a frame made of PVC. While the fish movement was restricted by the frame, care was taken
 345 to allow for sufficient room for gill movement. During the measurement the fish did not change posture. The fish
 346 holder was placed on a xy-slider made of PVC within the center of the electrode array. This setup allowed to adjust
 347 the fish to the same depths as the electrodes and to set the xy-position manually in reference to preset marks on
 348 the slider. In order to systematically measure the spatial distribution of the electric field, we kept the position of
 349 the electrodes constant and instead adjusted the fish's location. We sampled a grid with a total of 108 locations in
 350 18×6 steps using a resolution of 2×4.5 cm.

351 **Field monitoring system**

352 For field recordings we employed a recording system consisting of a custom-built, portable 64-channel elec-
 353 trode and amplifier system running on 12 V car batteries (Fig. 1 C – E). Electrodes are low-noise headstages en-
 354 cased in epoxy resin ($1 \times$ gain, $10 \times 5 \times 5$ mm). Signals detected by the headstages are fed into the main ampli-
 355 fier ($100 \times$ gain, 1st order high-pass filter 100 Hz, low-pass 10 kHz) and digitized with 20 kHz per channel
 356 with 16-bit using a custom-built low-power-consumption computer with two digital-analog converter-cards (PCI-
 357 6259, National Instruments, Austin, Texas, USA). Recordings were controlled with custom software written in
 358 C++ (<https://github.com/bendalab/fishgrid>) that also saved data to hard disk for offline analysis (full day
 359 recordings exceeding 400 GB of uncompressed data per day). Raw signals and power spectra were monitored
 360 online to ensure the quality of the recordings. We used a minimum of 54 electrodes, arranged in an 9×6 array cov-
 361 ering an area of 240×150 cm (30 cm spacing). The electrodes were mounted on a rigid frame (thermoplast 4×4 cm
 362 profiles, 60 % polyamid, 40% fiberglass; Technoform Kunststoffprofile GmbH, Lohfelden, Germany), which was
 363 submerged into the stream and fixed in height 30 cm below the water surface. Care was taken to position part of
 364 the electrode array below the undercut banks of the stream in order to capture the EODs of fish hiding in the root
 365 masses. The recording area covered about half of the width of the stream and the hiding places of several electric
 366 fish. The maximum uninterrupted recording time was limited to 14 hours, determined by the capacity of the car
 367 batteries (2×70 Ah) and the power consumption of the computer (22 W) and amplifier system (25 W). Facilities
 368 for charging the batteries were a bottleneck (solar power and gasoline-powered generators), therefore we focused
 369 on nighttime recordings. Gymnotiform species feature a cyclic reproduction controlled by environmental factors.
 370 In the tropics these factors are related to the transition from dry to wet season and include an increase in water level
 371 and a decrease in water conductivity (Kirschbaum and Schugardt, 2002). We therefore recorded EODs during the
 372 transition from dry to wet season in February, March, and May 2012 and acquired a total of 162 hours of data.

373 **Field site**

374 The field site is located in the Tuira River basin, Province of Darién, Republic of Panamá, at Quebrada La Hoya, a
 375 narrow and slow-flowing creek supplying the Chucunaque River. Data were recorded about 2 km from the Emberá
 376 community of Peña Bijagual and about 5 km upstream of the stream's mouth ($8^{\circ}15'13.50''\text{N}$, $77^{\circ}42'49.40''\text{W}$).
 377 The water of the creek is clear, but becomes turbid for several hours after heavy rainfall. The creek flows through
 378 a moist secondary tropical lowland forest, which, according to local residents, gets partially flooded on a regular
 379 basis during the wet season (May – November). The water levels of the creek typically range from 20 – 130 cm at
 380 different locations, but can rise temporarily to over 200 cm after heavy rainfall. At our recording site (fig. 1 E), the
 381 water level ranged from 20 – 70 cm. The banks of the creek are typically steep and excavated, consisting mostly
 382 of root masses of large trees. The water temperature varied between 25 and 27 °C on a daily basis and water
 383 conductivity was stable at 150 – 160 $\mu\text{S}/\text{cm}$. At this field site we recorded four species of weakly electric fish, the
 384 pulse-type fish *Brachyhyppopomus occidentalis* (~ 30 – 100 pulses per second), the wave-type species *Sternopygus*
 385 *dariensis* (EODf at ~ 40 – 220 Hz), *Eigenmannia humboldtii* (~ 200 – 600 Hz), and *Apteronotus rostratus* (~ 600
 386 – 1100 Hz).

387 **Data analysis**

388 All data analysis was performed in Python 2.7 (www.python.org, <https://www.scipy.org/>). Scripts and raw
 389 data (2.0 TB) are available on request, some of the core algorithms are accessible at [https://github.com/](https://github.com/bendalab/thunderfish)
 390 [bendalab/thunderfish](https://github.com/bendalab/thunderfish). Summary data are expressed as means \pm standard deviation, unless indicated other-
 391 wise.

392 **Consistency over time**

393 In order to create temporal consistency, we matched newly detected fish from the current analysis window to fish
 394 detected in recent analysis windows. If a fish with an EODf differing by less than 10 Hz was found in the previous

395 detections, the new data was added, otherwise the fish was treated as a new candidate. If this candidate was
 396 detected robustly in the following analysis windows, typically over several seconds, it was marked as a confirmed
 397 fish detection. Otherwise, it was discarded as a false detection.

398 **Estimation of electric fish location and orientation**

399 The EOD amplitude data used for the estimation of fish location and orientation was extracted from the envelopes
 400 of the bandpass-filtered voltage traces at the EOD f . For each detected fish the electrode's voltage traces were
 401 bandpass-filtered (Butterworth filter, 3rd order, $5 \times$ multi-pass, ± 7 Hz width) at the fish's EOD f . For each passband
 402 the signal envelope was estimated each 40 ms using a root-mean-square filter over 10 EOD cycles multiplied by
 403 $\sqrt{2}$.

404 In the following we describe the three algorithms tested for fish localization.

Weighted spatial average A simple estimate of 2D fish location and orientation is based on a weighted spatial average. The fish position \vec{x} is estimated from n electrodes i with the largest envelope amplitudes A_i at position \vec{e}_i as a weighted spatial average, given by

$$\vec{x} = \frac{\sum_{i=1}^n \sqrt{A_i} \cdot \vec{e}_i}{\sum_{i=1}^n \sqrt{A_i}}. \quad (1)$$

405 For the variant that uses only the four electrodes with the largest EOD amplitude, the position was computed only,
 406 if at least 2 electrodes with amplitudes greater than $15 \mu\text{V}$ were available. If at least 4 electrodes with amplitudes
 407 greater $1 \mu\text{V}$ were available, $n = 4$, otherwise $n = 2$. For the other variant that uses all electrodes n is set to the
 408 number of electrodes of the electrode array.

409 The EOD of a fish can cause a very large amplitude on nearby electrodes, because of the electric field's recip-
 410 rocal dependence on distance. This effect results in a relatively large localization error, if a simple weighted spatial
 411 average is used, because the position estimate is pulled towards the strongest electrode. The localization error is
 412 reduced by using the square-root of the EOD amplitude as a weight, $\sqrt{A_i}$, which reduces the impact of electrodes
 413 with large EOD amplitudes.

414 For approximating fish orientation, we first divided the electrodes into two subgroups of opposite polarity.
 415 Because the EOD amplitudes are extracted as absolute values, polarity information of the EOD on the respective
 416 electrodes is missing and has to be estimated in an additional analysis step. The polarity of the electrodes was
 417 determined by calculating the correlations of the electrodes' bandpass-filtered voltage traces (40 ms windows)
 418 relative to that of the electrode with the largest amplitude. Electrodes with correlations larger than $+0.9$ were
 419 assigned to one group and correlations smaller than -0.9 to the other. If both groups contained at least 4 electrodes,
 420 each group's center was estimated by calculating the weighted spatial average, Eq. 1. The direction of the vector
 421 connecting the centers of the two groups is an estimated of the orientation of the body axis of the fish.

Dipole model The potential generated by an ideal electric dipole at a distance r and an angle ϕ measured against the dipole moment is given by

$$\phi(r, \phi, P) = P \frac{\cos \phi}{r^2} \quad (2)$$

422 where P is the magnitude of the dipole moment divided by $4\pi\epsilon$ with ϵ being the permittivity of water.

Because the amplitude data fitted with this model are absolute values, we used the absolute value of Eq. (2). For estimating the position of a fish we fitted the dipole model Eq. (2) to the EOD amplitudes recorded by the electrode array. This is a numerically difficult minimization problem, because of the large number of local minima between the singularities at the positions of the electrodes. We therefore introduced a regularizer α in the denominator, to remove these singularities and make the problem numerically more stable. The search for a robust solution was improved by introducing an additional offset parameter β [JB: Was β fixed (what value?) or not?]. [JH: I think the value was lowered for sequential fit iterations. Will add the details.] Finally, we treated the exponent of the

power law as a free parameter q . Together, these modifications yield the regularized dipole function, given by

$$\phi(r, \varphi, P) = \left| P \frac{\cos \varphi}{r^q + \alpha} + \beta \right| \quad (3)$$

423 A weighted spatial average over all available electrodes was used to compute initial values for the optimization.
 424 The optimization was performed over two iterations using stepwise decreasing values for α (10^{-2} and 10^{-3}) and
 425 using the result of the first iteration as initial values for the last. The successful optimization directly yields the
 426 dipole's location, orientation, its moment's magnitude, and the potential distribution's effective power law. Since
 427 we are optimizing a function with 8 parameters [**JB: 9 if we also have β**], at least 8 data points, i.e. amplitude
 428 measurements from at least 8 electrodes, are necessary for a successful optimization.

429 **Simulations** [**JB: briefly explain how the simulations were done (was noise added?), and over what range and**
 430 **resolution the parameter were varied!**]

431 From the fish moving on a circle: To allow for comparison with noisy field data minute EOD amplitudes below
 432 $1 \mu\text{V}$ were excluded.

433 **Inference of travelled distance**

434 We calculated a conservative estimate of the distances travelled from the median timepoints of upstream and down-
 435 stream and the median swimming speeds of each species. The timepoint of return was calculated as: $\Delta t_{\text{return}} =$
 436 $(\Delta t_{\text{total}}) \times v_{\text{downstream}} / (v_{\text{downstream}} + v_{\text{upstream}})$. The travelled distance was then calculated as $\Delta t_{\text{return}} \times v_{\text{upstream}} / 100$,
 437 in meters.

438 **Estimation of EOD field characteristics**

439 The parameters governing the electric field's decay over distance can be estimated from the EOD's maximum
 440 amplitudes at a given distance. Because of the non-linear amplitude decrease over distance, errors introduced by
 441 the inaccuracy of location estimation are particularly noticeable at small distances. We therefore limit the fit to the
 442 distance range > 20 cm. Because the largest amplitudes are extracted as a substantial fraction of the data in each bin
 443 (5 or 20%), the method has an implicit bias to underestimate the EOD amplitude in comparison to the dipole model
 444 fit. Water conductivity influences the effective EOD amplitude, but not the exponent of the power law governing
 445 the decrease of EOD amplitude over distance.

446 We tested this method on data from simulations of moving fish (Fig. 7). For fish moving on the same vertical
 447 level as the electrode array, both power law exponent and EOD amplitudes are extracted accurately (Fig. ?? A, B),
 448 even if the fish was moving partially outside the array. In contrast, for fish moving vertically elevated (E–H),
 449 the proposed method profoundly underestimates both exponent and EOD amplitude. The cause of this effect can
 450 easily be determined from the amplitude distributions over distance (Fig. ?? C, D): for small distances, the largest
 451 amplitudes of elevated fish saturate on a low level and deviate greatly from those of fish on level with the electrodes.
 452 The distribution of the largest amplitudes could not be reproduced well by a simple power law function. This effect
 453 could be compensated by fitting the amplitude distribution over larger distances only. In case of the fish moving
 454 15 cm above the electrode array, a fit to distances > 50 cm yielded the exponent -1.62 and an EOD amplitude of
 455 28 mV m^2 , values that are close to the parameters used in the dipole model. For the data presented in Fig. 10 D we
 456 manually reviewed all datasets and excluded those that showed saturation within the fit range.

457 **References**

- 458 Bullock T (1970) The reliability of neurons. *J Gen Physiol* 55:565–584.
 459 Bullock T, H R, Scheich H (1972) The jamming avoidance response of high frequency electric fish. II. Quantitative
 460 aspects. *J Comp Physiol* 77:23–48.

- 461 Caputi A, Carlson B, Macadar O (2005) Electric organs and their control. In: Electoreception. Springer, pp.
462 410–451.
- 463 Dunlap K (2002) Hormonal and body size correlates of electrocommunication behavior during dyadic interactions
464 in a weakly electric fish, *Apteronotus leptorhynchus*. *Horm Behav* 41:187–194.
- 465 Dunlap K, Thomas P, Zakon H (1998) Diversity of sexual dimorphism in electrocommunication signals and its
466 androgen regulation in a genus of electric fish, *Apteronotus*. *J Comp Physiol A* 183:77–86.
- 467 Fotowat H, Harrison R, Krahe R (2013a) Statistics of the electrosensory input in the freely swimming weakly
468 electric fish *Apteronotus leptorhynchus*. *J Neurosci* 33:13758–13772.
- 469 Fotowat H, Harrison R, Krahe R (2013b) Statistics of the electrosensory input in the freely swimming weakly
470 electric fish *Apteronotus leptorhynchus*. *J Neurosci* 33:13758–13772.
- 471 Hagedorn M, Heiligenberg W (1985) Court and spark: electric signals in the courtship and mating of gymnotid
472 fish. *Anim Behav* 33:254–265.
- 473 Hopkins C (1973) Lightning as background noise for communication among electric fish. *Nature* 242:268–270.
- 474 Jun J, Longtin A, Maler L (2013) Real-time localization of moving dipole sources for tracking multiple free-
475 swimming weakly electric fish. *PLoS ONE* 8.
- 476 Kirschbaum F, Schugardt C (2002) Reproductive strategies and developmental aspects in mormyrid and gymnoti-
477 form fishes. *J Physiol Paris* 96:557–566.
- 478 Knudsen E (1974) Behavioral thresholds to electric signals in high frequency electric fish. *J Comp Physiol A*
479 91:333–353.
- 480 Knudsen E (1975) Spatial aspects of the electric fields generated by weakly electric fish. *J Comp Physiol A*
481 99:103–118.
- 482 Moortgat K, Keller C, Bullock T, Sejnowski T (1998) Submicrosecond pacemaker precision is behaviorally mod-
483 ulated: the gymnotiform electromotor pathway. *Proc Natl Acad Sci USA* 95:4684–4689.
- 484 Nelson ME, MacIver MA (1999) Prey capture in the weakly electric fish *Apteronotus albifrons*: sensory acquisition
485 strategies and electrosensory consequences. *J Exp Biol* 202:1195–1203.
- 486 Rodriguez-Munoz R, Bretman A, Slate J, Walling C, Tregenza T (2010) Natural and sexual selection in a wild
487 insect population. *Science* 328:1269–1272.
- 488 Smith G (2013) Evolution and hormonal regulation of sex differences in the electrocommunication behavior of
489 ghost knifefishes (Apteronotidae). *J Exp Biol* 216:2421–33.
- 490 Todd B, Andrews D (1999) The identification of peaks in physiological signals. *Comput Biomed Res* 32:322–335.
- 491 Triefenbach F, Zakon H (2003) Effects of sex, sensitivity and status on cue recognition in the weakly electric fish
492 *Apteronotus leptorhynchus*. *Anim Behav* 65:19–28.
- 493 Wright S, Nocedal J (1999) Numerical optimization, volume 2. Springer New York.
- 494 Zakon H, Oestreich J, Tallarovic S, Triefenbach F (2002) EOD modulations of brown ghost electric fish: JARs,
495 chirps, rises, and dips. *J Physiol Paris* 96:451–458.